Available online at www.sciencedirect.com
SCIENCE DIRECT®
Journal of Sound and Vibration 272 (2004) 109–124
JOURNAL OF SOUND AND VIBRATION
www.elsevier.com/locate/jsvi

Numerical simulation of active control of structural vibration and acoustic radiation of a fluid-loaded laminated plate

Sheng Li*, Deyou Zhao

Department of Naval Architecture, Dalian University of Technology, Dalian 116024, China

Received 17 July 2002; accepted 20 March 2003

Abstract

Active control of structural vibration and acoustic radiation of a fluid-loaded laminated plate is numerically studied. A finite element formulation is developed for modelling the dynamic behavior of the laminated plate integrated with piezoelectric layers and viscoelastic layer based on the first order shear deformation theory (FSDT). The Rayleigh integral on the plate surface is coupled with the derived finite element formulation to model acoustic fluid–structure interaction of the baffled laminated plate subjected to heavy fluid loading. Active damping control and active constrained layer damping (ACLD) control of structural vibration and acoustic radiation of the baffled fluid-loaded laminated plate with piezoelectric layers acting as active damping layers and viscoelastic layer acting as passive damping layer are formulated using the developed numerical method and negative velocity feedback control algorithm. The control performance of the active damping control and the ACLD control of structural vibration and acoustic radiation of a fluid-loaded plate is numerically evaluated. The results obtained demonstrate that the ACLD is more effective. The proposed model can be used for designing and predicting the control of structural vibration and acoustic radiation of a fluid-loaded laminated plate using active damping control and the ACLD treatment.

1. Introduction

Active control of structural vibration and sound radiation of fluid-loaded structures has become a very interesting research area. Several researches have been focused on active structural-acoustic control (ASAC) applied to fluid-loaded structures. The concept of ASAC [1–3] involves controlling the acoustic response of a fluid–structure system by applying oscillating force inputs directly to the structure. The concept is similar to active vibration control (AVC) since the

*Corresponding author. Tel.: +86-411-4707326-8331; fax: +86-411-4707337.
E-mail address: shengli@dlut.edu.cn (S. Li).

0022-460X/03/$ - see front matter © 2003 Elsevier Ltd. All rights reserved.
doi:10.1016/S0022-460X(03)00321-3

actuators are vibrational inputs applied directly on a flexible structure, but the goal of reducing acoustic response often differs from the goal of reducing a purely structural response. ASAC also differs from active noise control (ANC), since ASAC applies vibrational inputs to structure itself rather than exciting the acoustic medium with loudspeakers. Gu and Fuller [4] analytically studied the active control of sound radiation from a simply supported rectangular fluid-loaded plate and determined the control forces by the optimal solution of a quadratic cost function. Meirovitch [5] used the non-linear Riccati equation to get optimal control to reduce the sound radiation pressure. Ruckman and Fuller [6] investigated the active control of acoustic radiation from a fluid-loaded spherical shell using linear quadratic optimal control theory. Lee and Park [7] used a near-field approach to active control of sound radiation from a fluid-loaded rectangular plate based on quadratic cost function.

Active control methods have emerged as a very promising method to reduce structural vibration and structural radiated noise at low frequencies and have been found to be complementary to passive control methods, which are good at high frequencies. Active–passive hybrid systems that integrate active actuators with significant, well-designed passive devices have been of popular interest to structural control researchers in recent years. Such an approach can compensate for system uncertainties through feedback actions and is more effective than a fixed passive design. On the other hand, it normally requires less control power than purely active systems. Also, since energy is always being dissipated, it is more stable than the active approach. In other words, it has the advantages of both the purely passive (stable, fail-safe, lower power consumption) and active (high performance, feedback actions) systems. Important among these systems is the active constrained layer damping (ACLD) treatment. The ACLD systems have been studied by various researchers [8–10]. It has been shown that the active component can provide adjustable damping, whereas the passive component can enhance gain and phase margins, reliability, practicality and high-frequency performance. An ACLD system generally consists of a piece of passive viscoelastic damping material (VEM) sandwiched between an active piezoelectric layer and the host structure.

The combination of active control technique in conjunction with new developments in specialized actuator and sensor materials has permitted the implementation of the concept of smart structure. Recent studies on smart structures have shown that piezoelectric materials can be an effective alternative to the conventional discrete sensing and control system. Bonding or embedding piezoelectric materials in a structure can act as sensors and actuators because of the direct and converse piezoelectric effects, respectively. Finite element models have been proposed [11–20] for analyzing the static and dynamic performance of such smart structures.

The present study is focused on active control of structural vibration and acoustic radiation of a baffled laminated composite plate with heavy fluid on one side. A finite element formulation is developed for modelling the dynamic behavior of the laminated plate integrated with piezoelectric layers and viscoelastic layer based on the first order shear deformation theory (FSDT). The Rayleigh integral on the plate surface is coupled with the derived finite element formulation to model acoustic fluid–structure interaction of the fluid-loaded laminated plate. The active damping control and the ACLD control of structural vibration and acoustic radiation of the baffled laminated plate with piezoelectric layers acting as active damping layer and viscoelastic layer acting as passive damping layer are formulated using negative velocity feedback control algorithm. The static response of a piezoelectric bimorph beam to electrical loading and the

natural frequencies of a cantilever beam with an active layer are calculated and compared with solutions of previous studies to demonstrate the reliability and the accuracy of the developed finite element model. The acoustic response of a stiffened plate in water is calculated to validate the developed numerical method for coupled fluid–structure interaction analysis. The control performance of the active damping control and the ACLD control of structural vibration and acoustic radiation of the baffled laminated plate is numerically studied based on the proposed model.

2. Theory

2.1. Structure—finite element method

A laminated composite plate with integrated piezoelectric sensors and actuators is shown in Fig. 1. It is assumed that the surfaces of the piezoelectric layers that are in contact with the substrate are suitably grounded. The piezoelectric layer is polarized in the thickness direction and exhibits transversely isotropic properties in the xy plane. The finite element formulation is developed using a four-noded two-dimensional quadrilateral isoparametric element shown in Fig. 2 [14]. The element is based on the first order shear deformation theory and has five degrees of freedom (d.o.f.): u, v, w, θ_x and θ_y at four nodes. Two additional d.o.f.s φ_s and φ_a per element are included to represent the electrical voltages of two different piezoelectric layers. For every additional piezoelectric layer an additional voltage d.o.f. is needed per element. The electric potential is constant throughout the plane of the element and varies linearly through the thickness of the piezoelectric layers. Using Hamilton's principle and the element, the overall system equations are obtained in terms of the global co-ordinate representing the global generalized mechanical displacement $\{d\}$, and the electric potentials, on the sensors $\{\varphi_s\}$, and on the actuators $\{\varphi_a\}$ as follows [16]:

$$[M]\{\ddot{d}\} + [K_{dd}]\{d\} - [K_{da}]\{\varphi_a\} - [K_{ds}]\{\varphi_s\} = \{F\}, \tag{1}$$

$$[K_{ad}]\{d\} + [K_{aa}]\{\varphi_a\} = \{q\}, \tag{2}$$

$$[K_{sd}]\{d\} + [K_{ss}]\{\varphi_s\} = \{0\}, \tag{3}$$

where $[M]$ is the global mass matrix, $[K_{dd}]$, $[K_{aa}]$ and $[K_{ss}]$ represent the global generalized stiffness matrices corresponding to the vectors of mechanical displacements, the actuator and the sensor potentials, respectively. The matrices $[K_{da}]$ and $[K_{ds}]$ are the electrical–mechanical coupling

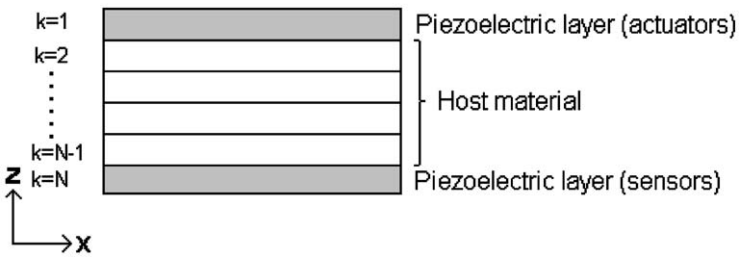

Fig. 1. Schematic of a laminated piezoelectric composite plate.

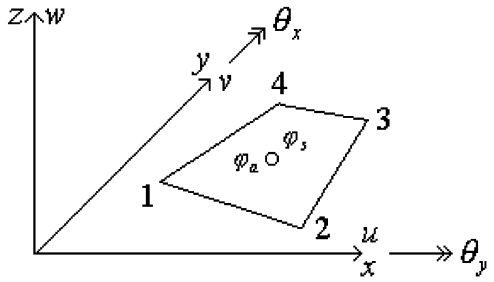

Fig. 2. Plate element with two additional electrical degrees of freedom.

stiffness matrices of the substrate and the piezoelectric actuator and sensor layers. $[K_{ad}] = [K_{da}]^{\mathrm{T}}$, $[K_{sd}] = [K_{ds}]^{\mathrm{T}}$. $\{F\}$ is the mechanical force vector. $\{q\}$ is the electric force vector as a result of the applied surface charge density distribution on the actuators.

The spatial distribution of electric potential on the sensor surface is obtained in terms of the mechanical displacement co-ordinates through electroelastic coupling from Eq. (3) as follows

$$\{\varphi_s\} = -[K_{ss}]^{-1}[K_{sd}]\{d\}. \tag{4}$$

In practice, the electric potential distribution is known on the actuators. In such cases, the global system Eq. (1) can be expressed in terms of the generalized mechanical displacement co-ordinates with the known electric potential distribution on the actuator surface appearing as external forcing through electroelastic coupling $[K_{da}]$

$$[M]\{\ddot{d}\} + [K]\{d\} = \{F\} + [K_{da}]\{\varphi_a\}, \tag{5}$$

where

$$[K] = [K_{dd}] + [K_{ds}][K_{ss}]^{-1}[K_{sd}]. \tag{6}$$

With the control algorithm known, $\{\varphi_a\}$ can be expressed in terms of $\{d\}$ and thus all the electric d.o.f.s in Eq. (5) can be condensed.

For active damping, negative velocity feedback can be adopted as the control algorithm. Velocity feedback is seen to be more robust control strategy than displacement or acceleration feedback, as far as unmodelled phase shifts are concerned [3]. The unmodelled phase shift is one of the most important effects which limit the performance of feedback controllers in practical mechanical systems. The phase shift may arise because of the dynamic response of the sensors or actuators being used or may be due to time delays in the controller.

Using the negative velocity feedback, $\{\varphi_s\}$ and $\{\varphi_a\}$ can be related by a control gain matrix $[G_{ain}]$, namely,

$$\{\varphi_a\} = -[G_{ain}]\{\dot{\varphi}_s\} = [G_{ain}][K_{ss}]^{-1}[K_{sd}]\{\dot{d}\}. \tag{7}$$

It should be noted that not the full state of the velocity $\{\dot{d}\}$ must be measured in Eq. (7) and measurement depends on the configuration of the sensors. As we know, non-full state measurement is of sensor placement problems and the question of sensor and actuator location is of specific importance. In practice it is useful to investigate possible sensor and/or actuator locations and to evaluate their impact on the closed-loop performance for purpose of control. However, the sensor and actuator placement problems and their importance have been studied

and emphasized in many investigations and contributions [20,21] and are not considered in this analysis. It is also clear that the above control algorithm ignores the measurement noise.

With Eq. (7), Eq. (5) becomes

$$[M]\{\ddot{d}\} + [\bar{C}]\{\dot{d}\} + [K]\{d\} = \{F\}, \tag{8}$$

where $[\bar{C}]$ is the active damping matrix

$$[\bar{C}] = [K_{da}][G_{ain}][K_{ss}]^{-1}[K_{sd}]. \tag{9}$$

For the ACLD treatment shown in Fig. 3, the negative velocity feedback can also be adopted as the control algorithm. The viscoelastic layer in Fig. 3 is assumed to be linearly viscoelastic and characterized by a complex modulus model. In such cases, Eq. (5) can be expressed as

$$[M]\{\ddot{d}\} + [\bar{C}]\{\dot{d}\} + \left[[K] + \mathrm{i}[K_{ve}^{'}]\right]\{d\} = \{F\}, \tag{10}$$

where $[\bar{C}]$ is the active damping matrix produced by the piezoactuator layer, $\mathrm{i} = (-1)^{1/2}$, $[K_{ve}^{'}]$ is the passive structural damping matrix caused by the viscoelastic layer.

Taking account of the Rayleigh's damping and structural damping of the laminated plate, Eq. (10) becomes

$$[M]\{\ddot{d}\} + \left[[C_R] + [\bar{C}]\right]\{\dot{d}\} + \left[[K] + \mathrm{i}[K^{'}]\right]\{d\} = \{F\}, \tag{11}$$

where $[C_R]$ is the Rayleigh's damping matrix, $[C_R] = \alpha[M] + \beta[K]$, in which α and β are the Rayleigh's damping coefficients, $[K^{'}]$ is the total structural damping matrix mainly produced by the viscoelastic layer.

For the case of harmonic excitation of frequency ω, Eq. (11) can be written as

$$\left(-\omega^2[M] + \mathrm{i}\omega\left[[C_R] + [\bar{C}]\right] + \left[[K] + \mathrm{i}[K^{'}]\right]\right)\{u\} = \{f\}, \tag{12}$$

or

$$\left(\mathrm{i}\omega[M] + \left[[C_R] + [\bar{C}]\right] + \frac{[K^{'}]}{\omega} + \frac{[K]}{\mathrm{i}\omega}\right)\{v\} = \{f\}, \tag{13}$$

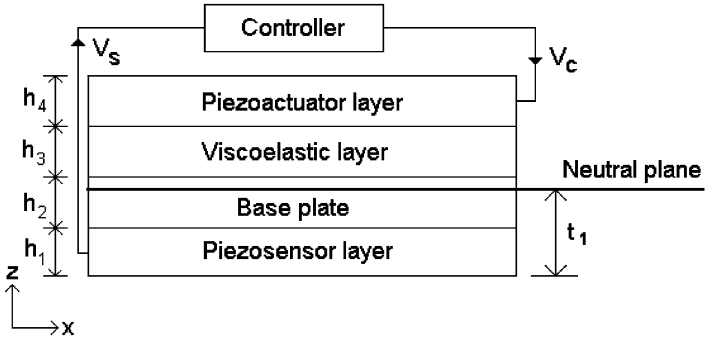

Fig. 3. A plate with ACLD treatment.

where $\{u\}$ is the complex amplitude of the displacement vector for all structural d.o.f., $\{v\} = \mathrm{i}\omega\{u\}$ is the complex amplitude of the velocity vector, $\{f\}$ is the complex amplitude of the vector of mechanical forces applied to the structure.

2.2. Sound radiation—the Rayleigh integral

For a harmonically vibrating plate surface extending over an infinite half-space, the acoustic pressure at any field point P according to the Rayleigh integral can be described as follows [22]

$$p(P) = \mathrm{i}\omega\rho \int_S \mathrm{e}^{-\mathrm{i}kr} v_n(Q)/2\pi r \,\mathrm{d}S, \tag{14}$$

where $p(P)$ is the acoustic pressure at the field point P, $v_n(Q)$ is the normal velocity of the vibrating surface at a point Q on the plate surface, $r = |Q - P|$, ρ is the density of the fluid, $k = \omega/c$ is the acoustic wavenumber, c is the speed of sound in the fluid, S is the plate surface.

Discretisizing the plate surface into four-noded two-dimensional quadrilateral isoparametric elements and interpolating the structural normal velocity and surface pressure over each element allow Eq. (14) (for $P \in S$) to be written in terms of the nodal normal velocity $\{v_n\}$ and surface pressure $\{p\}$ as

$$\{p\} = [D]\{v_n\}, \tag{15}$$

where $[D]$ is the acoustic impedance matrix. In the calculation of $[D]$ the integrand in Eq. (14) (for $P \in S$) is singular and the singular integral should be accurately evaluated [23,24]. This equation provides the link between the acoustic pressure and normal velocity on the plate surface.

2.3. Active control of coupled system

When a structure is loaded only with air in a free space, the structural and acoustic models are solved independently. However, in the case of a structure immersed in water, due to the fluid impedance is comparable to that of the structure, the structural and acoustic systems are strongly coupled and must be solved simultaneously.

The structural and acoustic systems are coupled together by considering the acoustic pressure acting on the surface of the structure as an additional external load vector $\{f_p\}$. The load vector, which can be found by application of Hamilton's principle, is given by

$$\{f_p\} = \int_S [N]^{\mathrm{T}} p \,\mathrm{d}S, \tag{16}$$

where $[N]$ is a matrix of interpolation function, the superscript T denotes the matrix transpose. Since the acoustic pressures are known only at the nodal locations, they are mapped across the element by the interpolation functions during the integration in Eq. (16). Hence, the acoustic load vector is written in matrix form

$$\{f_p\} = [G][A]\{p\}, \tag{17}$$

where $[A] = \int_S [N]^{\mathrm{T}}[N] \,\mathrm{d}S$ and $[G]$ is the transformation matrix to transform a vector of normal forces to a vector of forces to all structural d.o.f.

Thus, the global dynamic equation of coupled system with active control is formed as

$$\left(\mathrm{i}\omega[M] + \left[[C_R] + [\bar{C}]\right] + \frac{[K']}{\omega} + \frac{[K]}{\mathrm{i}\omega}\right)\{v\} = \{f\} - [G][A]\{p\}. \tag{18}$$

The vector of normal velocity $\{v_n\}$ in Eq. (15) is related to the vector of the structural velocity $\{v\}$ by the transformation matrix $[G]$

$$\{v_n\} = [G]^{\mathrm{T}}\{v\}. \tag{19}$$

If velocities $\{v_n\}$ and $\{v\}$ are eliminated from Eqs. (15), (18) and (19), the resulting equation for the coupled fluid–structure system is

$$\left([I] + [D][G]^{\mathrm{T}}[Z]^{-1}[G][A]\right)\{p\} = [D][G]^{\mathrm{T}}[Z]^{-1}\{f\}, \tag{20}$$

where $[I]$ is the identity matrix

$$[Z] = \left(\mathrm{i}\omega[M] + \left[[C_R] + [\bar{C}]\right] + \frac{[K']}{\omega} + \frac{[K]}{\mathrm{i}\omega}\right).$$

Once system Eq. (20) has been solved in terms of the surface pressure $\{p\}$, the structural velocity $\{v\}$ and the normal velocity $\{v_n\}$ may be recovered by solving Eqs. (18) and (19).

The mean square velocity $\langle \bar{v}_n^2 \rangle$ and the acoustic power Π of the plate can be calculated from the following formulas

$$\langle \bar{v}_n^2 \rangle = \frac{1}{2S_0}\int_S |v_n|^2 \,\mathrm{d}S, \tag{21}$$

where S_0 is the area of the plate.

$$\Pi = \frac{1}{2}\int_S \mathrm{Re}(pv_n^*)\,\mathrm{d}S, \tag{22}$$

where the asterisk denotes the complex conjugate.

3. Numerical results and discussion

In this section, first the static response of a piezoelectric bimorph beam to electrical loading and the natural frequencies of a cantilever beam with an active layer are calculated and compared with solutions of previous studies to demonstrate the reliability and the accuracy of the developed finite element model. Second, the acoustic response of a stiffened plate in water is calculated to validate the developed numerical method for coupled fluid–structure interaction analysis. Finally, the performance of the active damping control and the ACLD control of structural vibration and acoustic radiation in water of the baffled laminated plate is studied.

3.1. Bimorph beam

A cantilevered piezoelectric bimorph beam is shown in Fig. 4. It consists of two identical PVDF layers ($E = 2\,\mathrm{GPa}$, $v = 0.29$, $e_{31} = 0.046\,\mathrm{C/m^2}$, $\xi_{33}^S = 0.1062\,\mathrm{nF/m}$) with vertical but opposite polarities and, hence, will bend when an electric field is applied vertically. The bimorph beam is modelled by 5 and 20 elements, respectively, along the length. With a unit voltage applied across

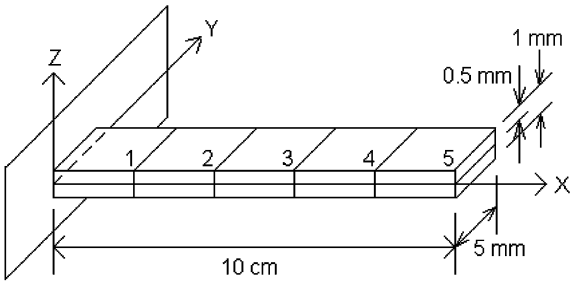

Fig. 4. A cantilevered piezoelectric bimorph beam.

Table 1
Static deflection of the piezoelectric bimorph beam (10^{-7} m)

	Distance x (mm)				
	20	40	60	80	100
Tzou [25] (analytical)	0.138	0.552	1.242	2.208	3.450
Detwiler et al. [14] (plate element)	0.14	0.55	1.24	2.21	3.45
Tzou and Ye [26] (solid-shell element)	0.132	0.528	1.19	2.11	3.30
Present (5 elements)	0.145	0.562	1.238	2.176	3.374
Present (20 elements)	0.137	0.535	1.195	2.116	3.299

the thickness, the deflection of bimorph beam is computed by the present plate element and compared with the theoretical and other finite element predictions as listed in Table 1. It can be seen that the results obtained by the present plate element are in good agreement with other predications.

3.2. Laminated piezoelectric composite beam

The beam shown in Fig. 5 has aluminum as substrate along with an adhesive layer and a piezoceramic layer (PZT-4). The material properties are: $E_{PZT} = 83.0\,\text{GPa}$, $E_{adh.} = 6.9\,\text{GPa}$, $E_{Al} = 68.9\,\text{GPa}$, $v_{PZT} = 0.31$, $v_{adh.} = 0.4$, $v_{Al} = 0.25$, $\rho_{PZT} = 7600\,\text{kg/m}^3$, $\rho_{adh.} = 1662\,\text{kg/m}^3$, $\rho_{Al} = 2769\,\text{kg/m}^3$, $e_{31} = -10.126\,\text{C/m}^2$, $\xi_{33}^S = 11.53\,\text{nF/m}$. The neutral axis can be determined by considering the force balance in the longitudinal direction [10] as $t_1 = 8.5586\,\text{mm}$. The beam is modelled by 1×6 and 3×15 elements. The computed natural frequencies given in Table 2 show convergence and good agreement with the results reported by Raja et al. [19], Saravanos and Heyliger [27] and Robbins, Reddy [28].

3.3. Acoustic radiation of a fluid-loaded stiffened plate

The simply supported square plate (dimension $a = 1\,\text{m}$) of thickness $h = 5\,\text{cm}$, reinforced by four stiffeners of rectangular cross-section located as shown in Fig. 6. The depth and width of the stiffeners are $H = 7.5\,\text{cm}$ and $W = 5\,\text{cm}$, respectively. The plate and stiffeners material is steel ($\rho_s = 7850\,\text{kg/m}^3$, $E = 210.0\,\text{GPa}$, $v = 0.3$). A structural damping factor $\eta = 0.01$ is assumed for

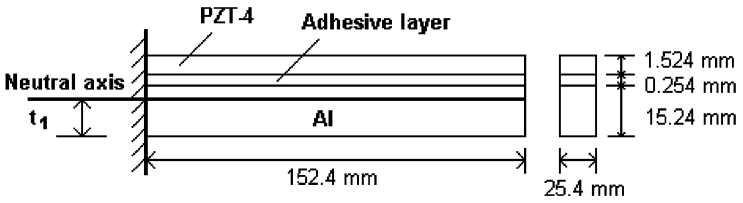

Fig. 5. A cantilever beam with an adhered piezoelectric layer.

Table 2
Natural frequencies of the cantilever

	Frequency (Hz)				
	1	2	3	4	5
Raja et al. [19]	533.3	3203.3	8467.5	15,490.4	23,854.1
Saravanos and Heyliger [27]	544.2	3242.0	8496.0	15,391.0	—
Robbins and Reddy [28]	538.4	3204.6	8395.5	15,196.7	22,632.7
Present (6 elements)	550.6	3259.1	8566.8	15,565.7	23,427.8
Present (45 elements)	552.7	3270.6	8490.8	15,186.0	22,776.3

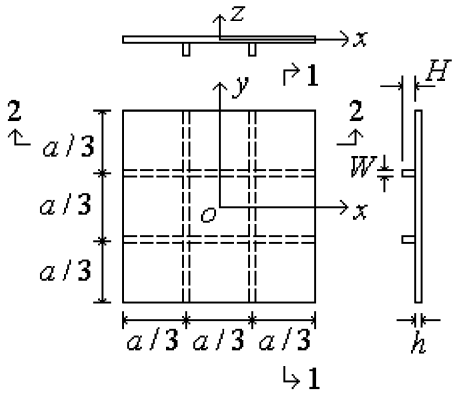

Fig. 6. Schematic of a stiffened plate.

both the plate and the stiffeners. The excitation is a transverse point force of magnitude $F_0 = 1$ N located at $x_0 = 7.5$ cm, $y_0 = 7.5$ cm. The values of density and acoustic velocity are $\rho = 1.21\,\mathrm{kg/m^3}$ and $c = 343$ m/s in air and $\rho = 1000\,\mathrm{kg/m^3}$ and $c = 1500$ m/s in water. The plate is modelled by 15×15 plate elements described in Section 2.1 and four stiffeners are modelled by 4×15 Timoshenko beam elements [29] and the eccentricity of the stiffeners is taken into account by a transformation that makes beam d.o.f. "slave" to "master" d.o.f. in the plate. Although this eccentric beam modelling may introduce an incompatibility and cause an error, Gupta and Ma [30] pointed out the error can be confined within an acceptable limit with a relatively few number of elements. The Rayleigh integral on the plate surface is made by discretisizing the plate surface into the same mesh as plate finite element mesh. This means that, for the acoustic radiation calculation, the stiffened plate is considered as being plane and only the "vibrating effect" of the

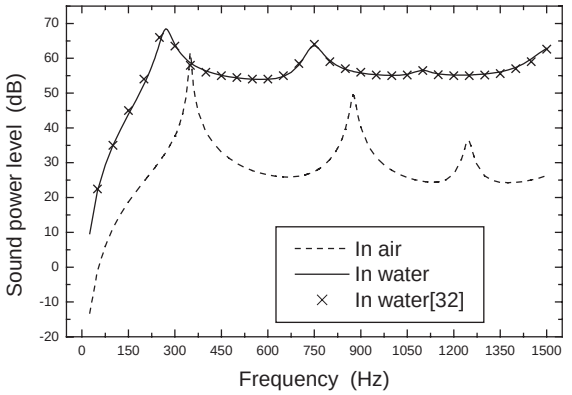

Fig. 7. Radiated sound power versus frequency.

Table 3
Natural frequencies of the stiffened plate in vacuo and in water

	Frequency (Hz)		
	1	2	3
Berry and Locqueteau [32] (in vacuo)	342	883	1271
Present (in vacuo)	349	875	1246
Present (in water)	272	763	1128

stiffeners is considered [31]. Fig. 7 shows the radiated sound power level (dB, re:10^{-12} W) of the stiffened plate in air and in water respectively. It is clear that the present results for sound power agree well with those presented by Berry and Locqueteau [32]. The first three natural frequencies of the stiffened plate in-vacuo and in water are given in Table 3. The natural frequency of the stiffened plate in water is calculated based on Everstine's method [33].

3.4. Active damping control and ACLD control of structural vibration and acoustic radiation

The numerical simulation is based on a laminated rectangular plate shown in Fig. 3. The dimensions of the simply supported plate are $L_x = 0.455\,\text{m}$, $L_y = 0.379\,\text{m}$. The disturbance is assumed to be a point force with amplitude $F_0 = 1\,\text{N}$ and located at $(x_1, y_1) = (0.11375\,\text{m}, 0.09475\,\text{m})$ as shown in Fig. 8. The base plate is steel ($E = 210.0\,\text{GPa}$, $v = 0.3$, $\rho_s = 7850\,\text{kg/m}^3$). The piezoceramic layer is PZT-4 ($E_{11} = 81.3\,\text{GPa}$, $E_{22} = 81.3\,\text{GPa}$, $E_{33} = 64.5\,\text{GPa}$, $G_{12} = 30.6\,\text{GPa}$, $G_{13} = 25.6\,\text{GPa}$, $G_{23} = 25.6\,\text{GPa}$, $v_{12} = 0.33$, $v_{13} = 0.43$, $v_{23} = 0.43$, $e_{31} = -5.20\,\text{C/m}^2$, $e_{32} = -5.20\,\text{C/m}^2$, $e_{33} = 15.08\,\text{C/m}^2$, $e_{24} = 12.72\,\text{C/m}^2$, $\xi_{11}^S = 13.054\,\text{nF/m}$, $\xi_{22}^S = 13.054\,\text{nF/m}$, $\xi_{33}^S = 11.505\,\text{nF/m}$, $\rho = 7600\,\text{kg/m}^3$). The viscoelastic layer is 3M ISD112 ($G = 10(1 + \text{i})\,\text{MPa}$, $v = 0.499$, $\rho = 1600\,\text{kg/m}^3$). The laminated plate is modelled by 16×16 elements, as shown in Fig. 8. To control the structural vibration and acoustic radiation of the plate, the collocated sensors and actuators should be coupled into sensor/actuator (S/A) pairs through closed control loops. Then, the piezoelectric sensor/actuator layer is also modelled into

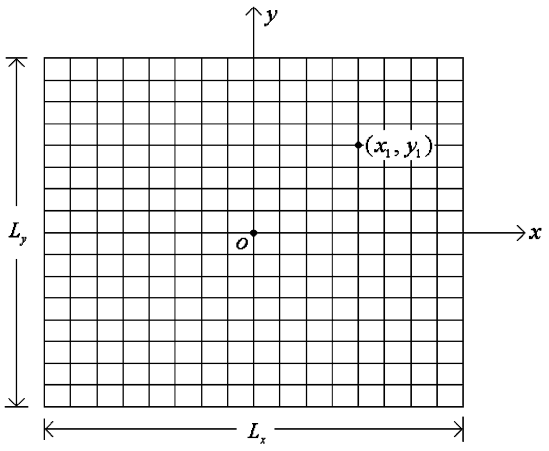

Fig. 8. Schematic of disturbance location and element mesh of plate.

Table 4
Natural frequencies of plates in vacuo and in water

Cases	Frequency (Hz)				
	1	2	3	4	5
Case A: Base plate					
In vacuo	86.7	193.4	241.0	344.6	373.6
In water	30.5	94.0	121.7	193.7	210.4
Case B: Base plate+two piezoelectric layers					
In vacuo	105.5	235.2	293.0	418.8	454.1
In water	45.7	136.6	175.9	275.3	298.5
Case C: Base plate+two piezoelectric layers+viscoelastic layer					
In vacuo	155.5	346.4	431.5	616.2	668.1
In water	70.7	209.0	268.9	418.5	453.8

16×16 piezoelectric sensor/actuator pairs, as shown in Fig. 8. That is, each sensor/actuator patch has dimensions of about $0.028\,\text{m} \times 0.023\,\text{m}$. It should be noted that the piezoelectric PZT or PVDF used as sensor/actuator has a "breakdown" voltage [11]. The PVDF and PZT have different breakdown voltages and depend on their thickness. The maximum electrical field for PVDF and PZT is about $40\,\text{V}/\mu\text{m}$ and $2\,\text{V}/\mu\text{m}$, respectively.

Three cases of the laminated plate shown in Fig. 3 are considered as follows: Case A (Base plate, no control): $h_1 = h_3 = h_4 = 0.0\,\text{m}$, $h_2 = 0.003\,\text{m}$; Case B (Base plate + two piezoelectric layers, active damping control): $h_1 = h_4 = 0.001\,\text{m}$, $h_2 = 0.003\,\text{m}$, $h_3 = 0.0\,\text{m}$, the control gain matrix $[G_{ain}]$ is assumed to be a constant gain G_{ain}; Case C (Base plate + two piezoelectric layers + viscoelastic layer, ACLD control): $h_1 = h_4 = 0.001\,\text{m}$, $h_2 = 0.003\,\text{m}$, $h_3 = 0.003\,\text{m}$, $t_1 = 0.0028\text{m}$, the control gain matrix $[G_{ain}]$ is assumed to be a constant gain G_{ain}. The first five natural frequencies of plates in vacuo and in water are shown in Table 4.

Figs. 9–12 show the mean square velocity level (dB, re: $1\,\text{m}^2/s^2$) and the acoustic power level for these three cases, in air and in water, respectively. It should be noted that the damping of the base

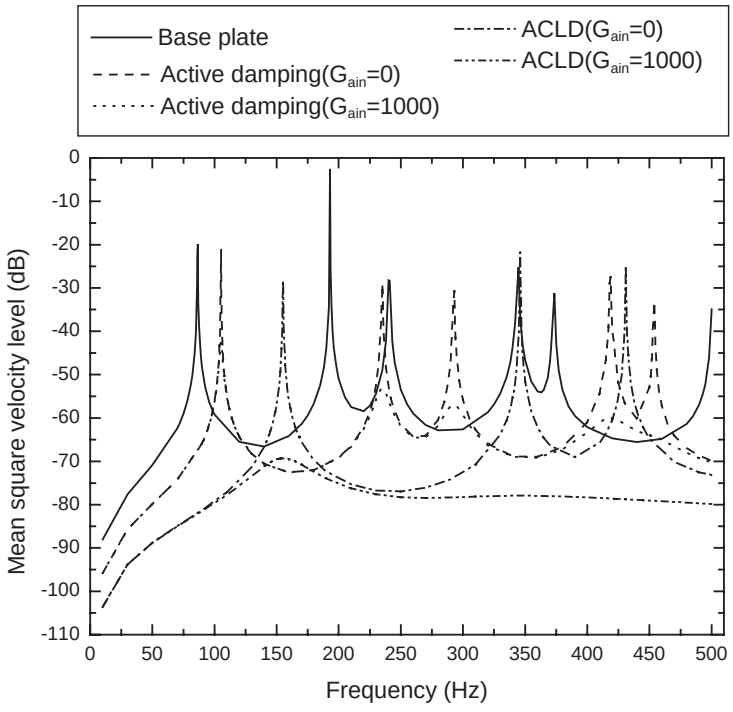

Fig. 9. Mean square velocity without control and with control of active damping and ACLD treatment (in air).

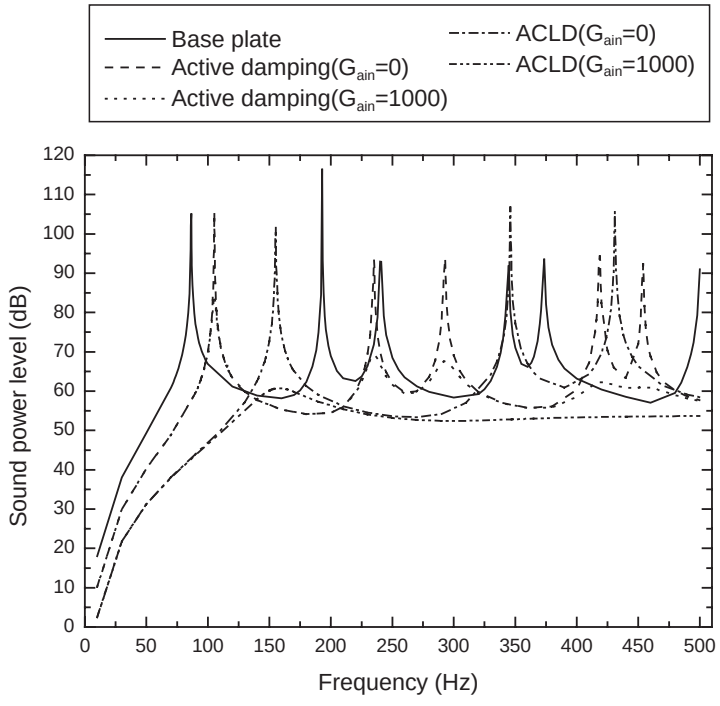

Fig. 10. Sound power without control and with control of active damping and ACLD treatment (in air).

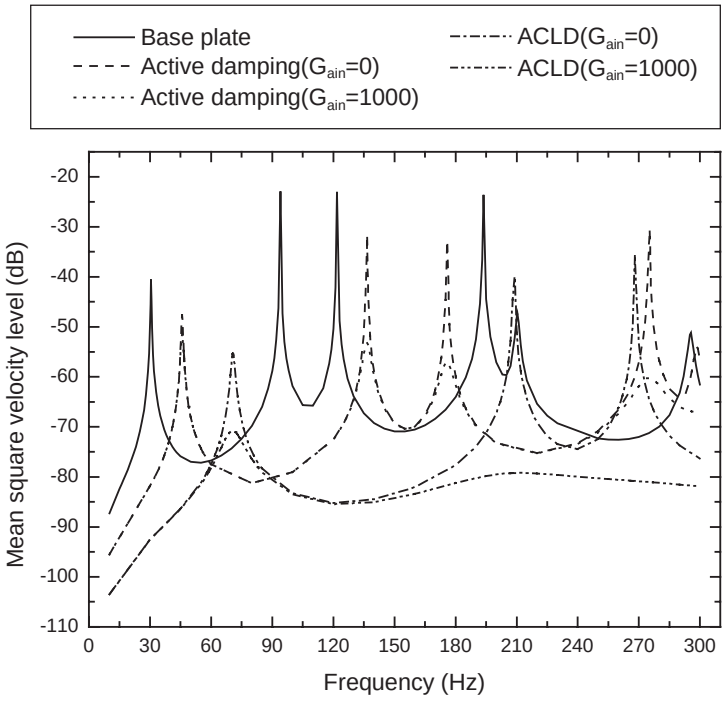

Fig. 11. Mean square velocity without control and with control of active damping and ACLD treatment (in water).

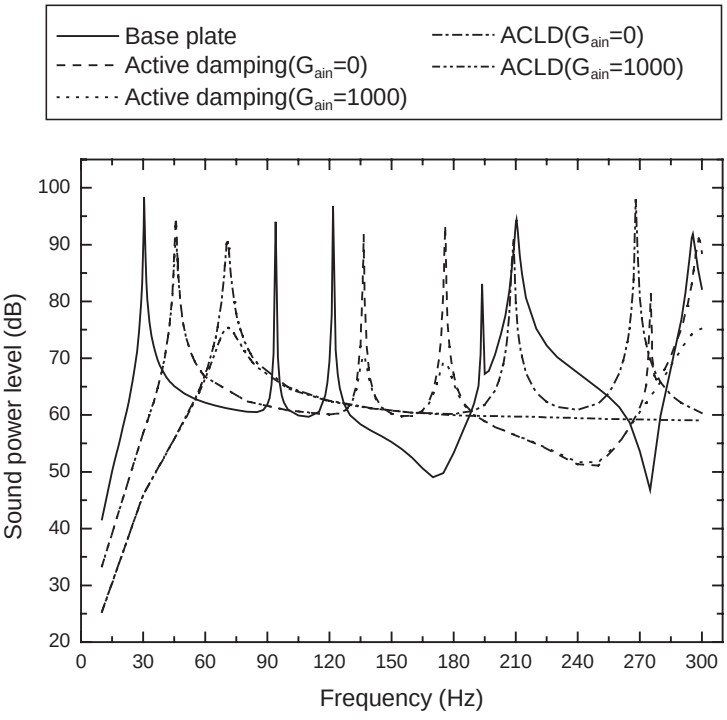

Fig. 12. Sound power without control and with control of active damping and ACLD treatment (in water).

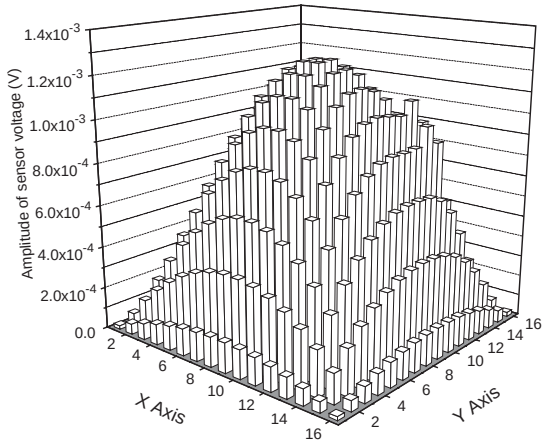

Fig. 13. Amplitude of sensor voltage of piezoelectric sheets for ACLD (in water, 70.7 Hz).

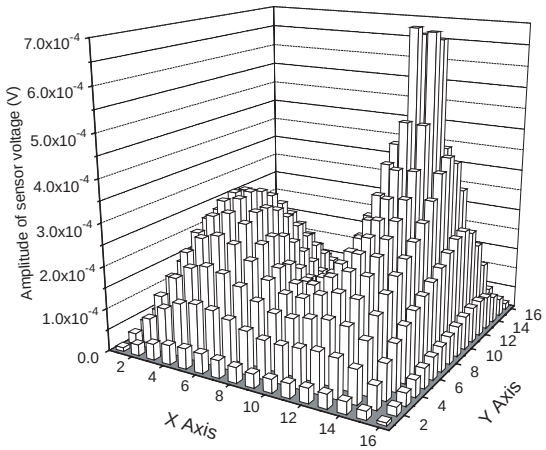

Fig. 14. Amplitude of sensor voltage of piezoelectric sheets for ACLD (in water, 209.0 Hz).

plate and the piezoelectric layer is not considered in the numerical results presented here. It is clear that there is a change of the natural frequency of the plate in the cases of no control, active damping control and ACLD control due to the effect of stiffness and mass of the piezoelectric layer and viscoelastic layer. This is apparent in Figs. 9–12 through the rightward shift to the resonance peaks of both the mean square velocity and the radiated power. It can be seen that the active damping control and the ACLD control can decrease the peak amplitude of the mean square velocity and the radiated sound power of the plate effectively and especially the ACLD control is more favorable for damping the structure to reduce vibration and sound radiation.

Figs. 13 and 14 show the distribution of electric potential on the sensor surface for ACLD at the first and second natural frequencies in water. For active control of time-harmonic problems using the negative velocity feedback with a constant gain G_{ain}, the amplitude of the control voltage on the piezoelectric actuator is related to the amplitude of the sensor voltage on the corresponding

piezoelectric sensor as $|\varphi_a| = G_{ain}\omega|\varphi_s|$. It means that with the same sensor voltage and control gain, the higher the excitation frequency is, the higher the control voltages need.

4. Conclusions

Active control of structural vibration and acoustic radiation of a fluid-loaded laminated plate is numerically studied. A finite element formulation is developed for modelling the dynamic behavior of the laminated plate integrated with piezoelectric layers and viscoelastic layer based on the first order shear deformation theory. The Rayleigh integral on the plate surface is coupled with the derived finite element formulation to model acoustic fluid–structure interaction of the fluid-loaded laminated plate. The active damping control and the ACLD control of structural vibration and acoustic radiation of the baffled laminated plate are formulated using negative velocity feedback control algorithm. Numerical simulations show that both the active damping control and the ACLD control can reduce the mean square velocity and the radiated sound power of the plate effectively and especially the ACLD control is more favorable for damping the structure to reduce vibration and sound radiation. The developed model provides a means for designing and predicting the performance of a fluid-loaded plate with different damping treatments that can be used in many engineering applications.

References

[1] C.R. Fuller, Active control of sound transmission/radiation from elastic plates by vibrational inputs. I. Analysis, *Journal of Sound and Vibration* 136 (1990) 1–15.
[2] C.R. Fuller, C.H. Hansen, S.D. Snyder, Active control of sound radiation from a vibrating rectangular panel by sound sources and vibration inputs: an experimental comparison, *Journal of Sound and Vibration* 145 (1991) 195–215.
[3] C.R. Fuller, S.J. Elliott, P.A. Nelson, *Active Control of Vibration*, Academic Press, San Diego, 1996.
[4] Y. Gu, C.R. Fuller, Active control of sound radiation from a fluid-loaded rectangular uniform plate, *Journal of the Acoustical Society of America* 93 (1993) 337–345.
[5] L. Meirovitch, A theory for the optimal control of the far-field acoustic pressure radiating from submerged structures, *Journal of the Acoustical Society of America* 93 (1993) 356–362.
[6] C.E. Ruckman, C.R. Fuller, Numerical simulation of active structural-acoustic control for a fluid-loaded spherical shell, *Journal of the Acoustical Society of America* 96 (1994) 2817–2825.
[7] H.K. Lee, Y.S. Park, A near-field approach to active control of sound radiation from a fluid-loaded rectangular plate, *Journal of Sound and Vibration* 196 (1996) 579–593.
[8] W.H. Liao, K.W. Wang, On the active-passive hybrid control actions of structures with active constrained layer treatments, *American Society of Mechanical Engineers Journal of Vibration and Acoustics* 119 (1997) 563–572.
[9] I.Y. Shen, A variational formulation a work-energy relation and damping mechanisms of active constrained layer treatments, *American Society of Mechanical Engineers Journal of Vibration and Acoustics* 119 (1997) 192–199.
[10] C.H. Park, A. Baz, Vibration control of bending modes of plates using active constrained layer damping, *Journal of Sound and Vibration* 227 (1999) 711–734.
[11] H.S. Tzou, C.I. Tseng, Distributed piezoelectric sensor/actuator design for dynamic measurement/control of distributed parameter systems: a piezoelectric finite element approach, *Journal of Sound and Vibration* 138 (1990) 17–34.
[12] S.K. Ha, C. Keilers, F.K. Chang, Finite element analysis of composite structures containing distributed piezoceramic sensors and actuators, *American Institute of Aeronautics and Astronautics Journal* 30 (1992) 772–780.

[13] W.S. Hwang, H.C. Park, Finite element modeling of piezoelectric sensors and actuators, *American Institute of Aeronautics and Astronautics Journal* 31 (1993) 930–937.
[14] D.T. Detwiler, M.-H.H. Shen, V.B. Venkayya, Finite element analysis of laminated composite structures containing distributed piezoelectric actuators and sensors, *Finite Elements in Analysis and Design* 20 (1995) 87–100.
[15] Changqin Chen, Xiaoming Wang, Yapeng Shen, Finite element approach of vibration control using self-sensing piezoelectric actuators, *Computers & Structures* 60 (1996) 505–512.
[16] B. Samanta, M.C. Ray, R. Bhattacharyya, Finite element model for active control of intelligent structures, *American Institute of Aeronautics and Astronautics Journal* 34 (1996) 1885–1893.
[17] K.Y. Sze, Y.S. Pan, Hybrid finite element models for piezoelectric materials, *Journal of Sound and Vibration* 226 (1999) 519–547.
[18] K.Y. Sze, L.Q. Yao, Modelling smart structures with segmented piezoelectric sensors and actuators, *Journal of Sound and Vibration* 235 (2000) 495–520.
[19] S. Raja, K. Rohwer, M. Rose, Piezothermoelastic modeling and active vibration control of laminated composite beams, *Journal of Intelligent Material Systems and Structures* 10 (1999) 890–899.
[20] G.R. Liu, X.Q. Peng, K.Y. Lam, Vibration control of simulation of laminated composite plates with integrated piezoelectrics, *Journal of Sound and Vibration* 220 (1999) 827–846.
[21] W. Gawronski, Actuator and sensor placement for structural testing and control, *Journal of Sound and Vibration* 208 (1997) 101–109.
[22] F. Fahy, *Sound and Structural Vibration: Radiation, Transmission and Response*, Academic Press, London, 1985.
[23] F.J. Rizzo, D.J. Shippy, An advanced boundary integral equation method for three-dimensional thermoelasticity, *International Journal of Numerical Methods in Engineering* 11 (1977) 1753–1768.
[24] F. Sgard, N. Atalla, J. Nicolas, Coupled FEM-BEM approach for mean flow effects on Vibro-acoustic behavior of planar structures, *American Institute of Aeronautics and Astronautics Journal* 32 (1994) 2351–2358.
[25] H.S. Tzou, *Piezoelectric Shells: Distributed Sensing and Control of Continua*, Kluwer, Dordrecht, 1993.
[26] H.S. Tzou, R. Ye, Analysis of piezoelectric structures with laminated piezoelectric triangle shell elements, *American Institute of Aeronautics and Astronautics Journal* 34 (1996) 110–115.
[27] D.A. Saravanos, P.R. Heyliger, Coupled layerwise analysis of composite beams with embedded piezoelectric sensors and actuators, *Journal of Intelligent Material Systems and Structures* 6 (1995) 350–363.
[28] D.H. Robbins, J.N. Reddy, Analysis of piezoelectrically actuated beams using a layer-wise displacement theory, *Computers & Structures* 41 (1991) 265–279.
[29] J.S. Przemieniecki, *Theory of Matrix Structural Analysis*, McGraw-Hill, New York, 1968.
[30] A.K. Gupta, P.S. Ma, Error in eccentric beam formulation, *International Journal of Numerical Methods in Engineering* 11 (1977) 1473–1477.
[31] S.L. Moyne, J.L. Tebec, J.C. Kraemer, Source effect of ribs in sound radiation of stiffened plates: experimental and calculation investigation, *Acustica* 86 (2000) 457–464.
[32] A. Berry, C. Locqueteau, Vibration and sound radiation of fluid-loaded stiffened plates with consideration of in-plane deformation, *Journal of the Acoustical Society of America* 100 (1996) 312–319.
[33] G.C. Everstine, Predication of low frequency vibrational frequencies of submerged structures, *American Society of Mechanical Engineers Journal of Vibration and Acoustics* 113 (1991) 187–191.